Activated carbon from agave wastes (agave tequilana) for supercapacitors via potentiostatic floating test

Isi Keyla Rangel-Heredia
Universidad Autonoma de Nuevo Leon Facultad de Ciencias Quimicas
Luis Carlos Torres-González (luis.torresgn@uanl.edu.mx)
Universidad Autonoma de Nuevo Leon Facultad de Ciencias Quimicas https://orcid.org/0000-0001-9212-4331
Eduardo Maximiano Sánchez-Cervantes
Universidad Autónoma de Nuevo León: Universidad Autonoma de Nuevo Leon
Lorena Leticia Garza-Tovar
Universidad Autónoma de Nuevo León: Universidad Autonoma de Nuevo Leon

Research Article

Keywords: Agave wastes, activated carbon, supercapacitor, potentiostatic floating test

Posted Date: April 2nd, 2021

DOI: https://doi.org/10.21203/rs.3.rs-232753/v1

Version of Record: A version of this preprint was published at Journal of Materials Science: Materials in Electronics on July 31st, 2021. See the published version at https://doi.org/10.1007/s10854-021-06649-0.

Abstract

To prepare an efficient supercapacitor, an activated carbon from agave wastes was prepared and their electrochemical performance was evaluated as a novel electrode for supercapacitor. The carbon was prepared by two thermal pyrolysis processes under nitrogen atmosphere. The first pyrolysis was achieved at 500°C until the charring of the bagasse, in the second pyrolysis step, the char was impregnated with different mass ratios of KOH (1:2 – 1:4) and thermally treated at 800 or 900°C, for 1 h under N_2 flow. The textural analysis showed that the activated carbon had a specific surface area of 1462 $m^2\ g^{-1}$ and depicted a type I isotherm (IUPAC) characteristic of a microporous carbon. Raman spectroscopy and XRD measurements confirm that the activated carbon contains a small graphitization degree and a disordered structure. The electrochemical study of the symmetric carbon supercapacitor was carried out in 1M Li_2SO_4 solution as the electrolyte. The electrochemical performance of the coin cell supercapacitor was evaluated under an accelerated ageing floating test consisting of potentiostatic steps at different voltages (1.5, 1.6 and 1.8 V) for 10 h followed by galvanostatic charge/discharge sequences, the overall procedure summarized a floating time up to 200 h. The highest capacitance was observed at a floating voltage of 1.5 V, with a large initial specific capacitance of 297 F g^{-1}.

Relevance Summary

In this article we propose a strategy to improve behavior in symmetric supercapacitors made from activated carbon based on agave wastes, that promises to be an interesting active material for supercapacitors, analyzing via potentiostatic floating test which presents major stability analysis of supercapacitor electrodes than traditional current charge-discharge cycling due to its low degradation in electrodes, respective characterizations of active material are also presented. Based on the results shown, was demonstrate a good performance after 150 h of floating test on activated carbon prepared from agave wastes (*Agave Tequilana*) from Arandas, México.

1. Introduction

In the last decade, much attention has been focused on the applications of different novel carbonaceous materials (agriculture waste, biomass, etc.) as electrode materials because of their low cost, high conductivity and unusual features. These materials are stable in diverse electrolytic solutions and are able to perform stable in a wide temperature range. [1]

A supercapacitor (SC) is an electrochemical energy storage device able to store charges in the electrode/electrolyte interface, SC demonstrate high power density and extended cycling life for energy applications, such as hybrid and electric vehicles, brake energy recovery systems, as well as to enhance the energy efficiency of instruments that require a peak power source, such as elevators, cranes, and locomotives [2-3]. The exploration for advances in SC technology is crucial to satisfy needs for the development of the future energy storage systems to help the use of sustainable energy sources, such as solar and wind electricity in agricultural areas, as well as an improved application of electric vehicles. In

order, to perform highly and constant electrical energy storage capacity and high specific power in SC [4-7], the electrodes fabricated from carbon materials [8] should have a microporous structure with elevated surface, high conductivity, propitious pore size distribution, and long cyclability [8-9].

Lately, the most stimulated research to increase the energy and power density of SC has been centred on novel carbon materials. However, advanced carbon materials, such as carbon nanotubes, graphene, [10] and resultant carbon from metal carbide have proved high capacitance and high-power density in electrochemical [11-13] and hybrid SC; those advanced carbonaceous materials would be considerably reduced by their high cost.

Electrode materials for SC have been substantially developed because of the increasing demand for a new type of electrical energy storage with a high specific power, good electrical conductivity and a long durability [14].

The most important advantage of these storage devices is the ability of a high dynamic charge propagation, which can be useful for the hybrid power sources, electrical vehicles, digital telecommunication systems, UPS (uninterruptible power supply) for computers, and pulse laser techniques. Another benefit of the electrochemical capacitor systems is the possibility of full discharge and that a short-circuit between the two electrodes is also not harmful [15]. The typical electrochemical accumulators cannot fulfill such demands due to the physicochemical processes and electrode polarization that go along with the chemical to electrical energy conversion.

Carbons derived from biomass (biomass carbon or biochar) have been applied as electrode materials in electrochemical energy systems. The major sources of biomass are residues coming from forest crops, agricultural crops, industry, domestic sources and marine wastes [16-18].

In the work reported by Xiao Li et al., they prepared a series of nanoporous carbons from sunflower seed shells by two different strategies and used them as electrode materials for electrochemical double layer capacitors (EDLC). The pore structure of the carbons depends on the activation temperature and dosage of KOH. The capacitive performances of these carbons were much better than ordered mesoporous carbons and commercial wood-based active carbon, which has been used due to its superior specific surface area electrode material for EDLC [19-21]. In this work, we prepared an activated carbon (AC) from agave wastes and tested as electrode for SC. This material in conjunction with the activating agent and the electrolyte seems to be very attractive precursors (cheap, abundant, etc.) to be used in SC, representing the novelty of the present work. The textural, structure and electrochemical performance of AC were investigated in detail.

2. Experimental

2.1 Preparation of activated carbon

The agave wastes for the study comes from the *Agave Tequilana* plants used in a tequila facility in Arandas, in central Mexico. This agave is the only **variety legally allowed for the tequila production.** The bagasse fibers were cut, weighted, and oven dried at 95 °C for 24 h. The first pyrolysis process was made under nitrogen at a temperature of 500 °C until charring (~ 6 to 12 h). The transformation into AC was achieved by a chemical activation process with KOH in a 1:4 (mass ratio), with a second pyrolysis step at 800 °C for 1 h under nitrogen flow. After activation, the carbon was first washed with 0.01 M HCl to remove ashes (inorganic materials) followed by washing with distilled water until reaching a neutral pH ~7. After that, carbon was dried at 105 °C for 2 h and stored in desiccators for further characterization.

2.2 Characterization

A Bruker D2 Phaser diffractometer was used for characterizing the carbonize fibers by XRD with Cu Kα radiation (λ = 1.5418 Å). The results of the Raman spectra were analyzed from AC samples employing a Raman Microscope, Thermo Scientific, with a 780 nm excitation laser. The specific surface area was obtained by the Brunauer–Emmett–Teller (BET) technique from the liquid nitrogen adsorption isotherm in a relative pressure ($P\ P_0^{-1}$) range of 0.01-1.0 with Quantachrome Company equipment, the pore volume and the pore size distribution were calculated by the Quenched Solid State Functional Theory (QSDFT) for Pore Size Analysis.

2.3 Electrochemical measurements

VMP300 Bio-Logic instrument was used to test the working potential window and electrochemical properties, all measurements were performed in air at room temperature. Electrodes were made by mixing carbon prepared in this work with carbon black acetylene, from Alfa Aesar and a 60 wt% dispersion of Polytetrafluoroethylene, from Aldrich, to make a paste with a weight ratio of 85:10:5 respectively. Paste was then dried at 65 °C in a vacuum oven. Analysis was tested in a two-electrode symmetric coin cell arrangement where each electrode had ~10 mg of mass and ~150 μm of thickness. Finally, cellulose filter paper was used to separate the electrodes and immersed in 1 M Li_2SO_4 solution as a neutral electrolyte.

The electrochemical behavior of the device was characterized before and after the floating test sequence by cyclic voltammetry (CV) and by electrochemical impedance spectroscopy (EIS), these measurements were made from 100 kHz to 0.01 Hz as the frequency range with 0 V of bias voltage and a potential amplitude of 10 mV.

For the accelerated ageing floating tests, experiments were carried out as follows: each sequence consisted of 10 h at maximum potentiostatic voltages (1.5, 1.6 and 1.8 V) and after every potentiostatic step, five galvanostatic charge discharge (GCD) cycles were applied under a 1 A g^{-1} of constant current. All periods of charge discharge cycles were reiterated twenty times with a total voltage holding time of 200 h. Specific capacitances were calculated for every 10 h stage at the fifth discharge curve, respectively (**Fig. 1**).

3. Results And Discussion

3.1 Structure and textural characterization

The XRD diffractogram (**Fig. 2**) shows a strong peak at 23° in 2θ and two weak peaks at 10° and 44° which reveals a typical pattern for an amorphous and disordered structure. To obtain more insight from the disorder structure a Raman spectroscopy analysis was carried out. **Fig. 3** shows the Raman spectra and as can be seen it shows two intense bands, at 1340 cm^{-1} (D band) and at 1560 cm^{-1} (G band) the presence of the characteristic G peak arises from the stretching of the C–C bond in graphitic materials and is usual to all sp^2 carbon materials [22]. The depicted D peak is due to lattice vibrations of the sp^2-sp^3 bonds of the amorphous carbon present in interstitial sites and the distorted graphitic lattice. It can be seen that the D peak shows a higher intensity compared to the G peak, with an intensity ratio of $R = (I_D\ I_G^{-1}) = 1.24$, that confirms the presence of a high degree of a disordered carbon material, as observe from the characteristic behavior of these peaks [23].

The surface texture of the AC was investigated by N_2 gas adsorption - desorption analysis, specific surface areas were determined via the BET method (S_{BET}). The N_2 adsorption and desorption isotherms for the AC are shown in **Fig. 4**. The analysis reveals a type I (b) isotherm according to IUPAC [24] for a microporous material. The isotherm is concave to the $P\ P_0^{-1}$ axis and the amount of adsorbed gas approaches without any limiting adsorption at high relative pressure ($P\ P_0^{-1}$). It is suggested that this type of isotherm could be found in microporous solids having a pore size distribution with a mixture of wide micropores and narrow mesopores instead of type I(a) isotherms that are found in microporous materials having mainly narrow micropores (< 1 nm) [24]. The textural properties of the AC are summarized in Table 1. The apparent BET reveals a high specific surface area value of 1460 $m^2\ g^{-1}$ and the total pore volume estimated was 0.69 $cm^3\ g^{-1}$, the mean pore width was found about 1.8 nm as shown in **Fig. 5**. For the QSDFT estimation of textural analysis a slit model pore was applied. It is worth to notice that the presence of micropores and mesopores are important for charge storage since micropores are responsible for ion traps during the energy storage and the mesopores act as channels for ion transport from the electrolyte to the interface between the electrode and electrolyte [25].

3.2 Electrochemical characterization

One way to raise the energy and power density in EDLCs is by increasing the cell voltage above 1.24 V of currently available EDLCs using AC. To analyze performance of the electrodes a symmetric SC device was prepared to carry-out electrochemical tests at three different operating voltages; 1.5, 1.6, and 1.8 V in 1M Li_2SO_4 solution as electrolyte and selected from previous CV experiments. Instead of using the long cycling charge-discharge performance test we carry out an alternative way known as potentiostatic floating test (or constant voltage hold test) more efficient for determination of the EDLCs stability limits [18-23]. This plot is sketched in figure 1 with 5 GCD cycles and 10 h of floating where for voltage tests and current are plotted. In the floating test, the capacitor is constantly exposed to voltage

values above the assumed stability limit. **Fig. 6a** shows at 1.5 V and 200 h, the behavior of a cell, indicating 25% decay in capacitance at 170 h, with a capacitance of 297 F g^{-1} calculated at the fifth cycle of every period, the capacitance loss of electrodes, it is possibly ascribed to higher potential in the positive electrode. On the other hand, the cell tested at 1.6 V and 200 h, it is possible to observe a 25% decay at 150 h with a capacitance of 285 F g^{-1}. Finally, for analysis at 1.8 V we can observe the shortest decay capacitance period of 25% at 90 h, indicating a capacitance of 264 F g^{-1} with a very high voltage and low stability, considering the extensively acceptable criteria for measuring end of life for SC (from 20% to 30% capacitance decay) [23]. The device at 1.5 V showed the greater stability and voltage hold for more hours, capacitance decay of 30% represents the point where SC reach their maximum active lifetime, this test was stopped at 110 h. For comparisons purposes in floating tests and according to other studies, by Bello et al., [7] their results showed capacitance loss of 25% with a constant voltage of 1.2 V for up to 120 h of voltage holding, in other cases the cell voltage increased above 2.5–2.8 V using electrolytes such as ionic liquids, with a decrease of the capacitance observed after 200 h of test at 3.75 V. The capacitance loss of 30% was observed after 340 h [14-16].

Fig. 6b illustrates the resistance according to the floating time, it was possible to notice that the resistance increased a 100% (1.4 Ω) at 150 h of voltage holding at 1.5 V. For the cell at 1.6 V, resistance increased 100% at 140 h and the cell tested at 1.8 V, showed that resistance increased rapidly at 75 h, as resistance increased a moderate degradation in the electrode occurred possibly associated to higher potential in the positive electrode [24-25]

This good electrochemical behavior could be ascribed to the micropore/mesopore distribution within the carbon material which provides the relevant pore sites accessible to electrolyte ions along with short diffusion paths supporting fast ions transport during the lengthy charge-discharge process [26-29]. Floating experiments were used to demonstrate stability in capacitors, as the time elapses, the electrode suffers degradation, and the advantage of an electric double layer capacitor is to increases the lifetime which allows it to be very stable above the nominal cell voltage and can be discharged to zero without harm as discussed previously in **Fig. 1**. [30]

Electrochemical impedance spectroscopy is a powerful technique that allows measuring both the equivalent resistance and the capacitance at different frequencies and helps to realize the performance of the electrode at open circuit potential or at any alternal current signal. Impedance measurements studies where performed with a voltage amplitude of 10 mV in a frequency range from100 kHz to 0.01 Hz. The Nyquist plot presented in **Fig. 6c** (red) exhibits a semicircle in the high to mid-frequency area which means the charge transfer resistance, it is also shown a vertical spike (line) in the low frequency area, which indicates an ideal capacitive behavior of carbon electrode material. Equivalent series resistance (ESR) originated from the total resistance of the electrolyte, the resistance of the active materials and the resistance at the interface between the active electrode material and current collector. The Nyquist plot after floating test it is also presented in **Fig. 6c** (black), showing a little deviation to the initial curve corroborating a minuscule deterioration of the AC electrode material. Before and after floating test in the Nyquist plots was observed comparable internal resistance values (ESR = 0.5 Ω and 1.1 Ω

respectively) shown in the figure, indicating a favorable contact between AC material and separators, current collectors and electrolyte. [31]

Fig. 6d presents the CV plots (20 mV) of the cell before and after voltage holding, showing an almost rectangular shape up to 1.5 V indicative of loss in capacitance as mentioned in **Fig. 6a** previous. The results observed in the CV plots evidently show that floating test does not have a notable degradation effect in the AC electrodes of the symmetric device.

Furthermore, it is acceptable to conclude the performance of the electrode material investigated presents successful and acceptable values, highlighting the promise of this material for electrochemical high power applications.

4. Conclusions

Carbon from agave wastes was activated with KOH showing a specific surface area of 1462 m^2 g^{-1} and depicted a type I (b) isotherm in the textural analysis, characteristic of microporous carbons. From the analyses of Raman spectroscopy and XRD allowed us to confirm that the AC included a small degree of graphitization and that its structure mostly consists of disordered carbon. Also, the performance of the symmetric carbon SC was carried out in a button cell at different maximum voltages of 1.5, 1.6 and 1.8 V followed by five galvanostatic charge/discharge cycles for a total voltage holding of 200 h. Further the cell capacitance was measured from the slope of every fifth discharge and the ESR from the discharge ohmic drop. The SC device that exhibits the highest capacitance and performance was observed with the cell at a floating voltage of 1.5 V, with a large initial specific capacitance of 297 F g^{-1} while in EIS was observed a capacitive performance before the floating test and after the analysis diffusive and resistance in material, it is possible describe this material with an ideal capacitive response for an energy storage device.

Declarations

Funding: Consejo Nacional de Ciencia y Tecnología **(**CONACYT) and Programa de Apoyo a la Investigación Científica y Tecnológica, Universidad Autónoma de Nuevo León (PAICYT-UANL)

Conflicts of interest: The authors declare that they have no known competing financial interests or personal relationships that could have appeared to influence the work reported in this paper.

Availability of data and material: The research group does not present any problems with the disposal of data and material

Code availability: Not applicable

Authors' contributions:

Isi keyla Rangel Heredia: Formal Analysis, Research, Writing – Original draft, Writing – Review & Editing

Luis Carlos Torres González: Conceptualization, Methodology, Writing – Review & Editing, Validation, Supervision, Project Administration, Funding Acquisition, Resources.

Eduardo Maximiano Sánchez Cervantes: Methodology, Validation, Writing – Review & Editing.

Lorena Leticia Garza Tovar: Conceptualization, Methodology, Validation & Writing.

Ethics approval: Approved

Consent to participate: Consent is approved by the research group

Consent for publication: Consent is approved by the research group

Acknowledgements

Authors would like to thank CONACYT (Consejo Nacional de Ciencia y Tecnología) and PAICYT-UANL (Programa de Apoyo para la Investigación Científica de la Universidad Autónoma de Nuevo León) for the financial research support to this project, IKRH would like to thank CONACYT for PhD scholarship-grant.

References

1. Ibrahim H, Ilinca A, Perron J (2008) Renewable and sustainable energy reviews 12 (5), 1221-1250
2. Nieto-Delgado C, Terrones M, Rangel-Méndez J (2011) Biomass and Bioenergy 35 (1), 103-112
3. Conway BE (1991) Electrochem Soc 138:1539
4. Chae J, Chen G (2012) Electrochim Acta 86, 248-254
5. Przygocki P, Abbas Q, Béguin F. (2018) Electrochim Acta, 269, 640-648
6. Ortiz-Bustos J, Real S, Cruz M, Santos-Peña J, (2017) Microporous and Mesoporous Mater 242, 221-230
7. Bello A, Barzegar F, Madito M, Momodu D, Khaleed A, Masikhwa A, Manyala N (2016) Electrochim Acta 213, 107-114
8. Abioye A, Ani, F, (2015). Renewable and sustainable energy reviews, 52, 1282-1293.
9. Laheäär A, Przygocki P, Abbas Q, Béguin F (2015) Electrochem Communications, 60, 21-25.
10. Kleszyk P, Ratajczak P, Skowron P, Jagiello J, Abbas Q, Frąckowiak E, Béguin F (2015) Carbon, 81, 148-157.
11. Salinas-Torres D, Shiraishi S, Morallón E, Cazorla-Amorós D (2015) Carbon, 82, 205-213.
12. Vaquero S, Palma J, Anderson M, Marcilla R (2013) J Electrochem Soc 160(11), A2064-A2069.
13. Kalyani P, Anitha A (2013 International J Hydrog Ener, 38(10) 4034-4045
14. Weingarth D, Foelske-Schmitz A, Kötz R. (2013) J Power Sourc225, 84-88.
15. Elmouwahidi A, Zapata-Benabithe Z, Carrasco-Marín F, Moreno-Castilla C (2012) Biores techn111 185-190.

16. Li X, Xing W, Zhuo S, Zhou J, Li F, Qiao S, Lu G (2011) Biores techno102(2) 1118-1123
17. Jain A, Balasubramanian R, Srinivasan M (2016) Chem Engineer J283, 789-805.
18. Schröder E, Thomauske K, Oechsler B, Herberger S (2011) In Progress in biomass and bioenergy production. IntechOpen.
19. Obreja V (2008) Phys E: Low-dimns Systms Nanostructs40(7), 2596-2605.
20. Gao Q (2013) Optimizing carbon/carbon supercapacitors in aqueous and organic electrolytes(Doctoral dissertation, Université d'Orléans)
21. Galiński M, Lewandowski A, Stępniak I (2006) Electrochim acta51(26), 5567-5580.
22. Shimodaira N, Masui A (2002) J Appl Phys92(2) 902-909
23. Wang H, Chung H, Liu W (2013) IEEE Transactions on Power Electronics29(3) 1163-1175
24. Momodu D, Madito M, Barzegar F, Bello A, Khaleed A, Olaniyan O, Manyala N (2017) J Solid State Electrochem21(3), 859-872
25. Thommes M, Kaneko K, Neimark A, Olivier J, Rodriguez-Reinoso F, Rouquerol J, Sing K (2015) Pure Appl Chem87(9-10) 1051-1069
26. Ohno H (2005) Electrochemical aspects of ionic liquids
27. Moganty S, Baltus R, Roy D (2009) Chem Phys Lett483(1-3), 90-94
28. Gao X, Xing W, Zhou J, Wang G, Zhuo S, Liu Z, Yan Z (2014) Electrochim Acta, 133, 459-466
29. Timperman L, Galiano H, Lemordant D, Anouti M (2011) Electrochem Comms13(10), 1112-1115
30. Lazzari M, Soavi F, Mastragostino M (2008) J Power Sources, 178(1), 490-496

Table

Table 1 - Textural Characterization of Activated Carbon (AC)

Parameter	Value
Total pore volume, V_t [$cm^3\ g^{-1}$]	0.69
Total volume of micropores, V_0 [$cm^3\ g^{-1}$]	0.48
Average pore size, L_0 [nm]	1.8
Apparent BET area, S_{BET} [$m^2\ g^{-1}$]	1462
Volume of mesopores, V_{meso} [$cm^3\ g^{-1}$]	0.21

Figures

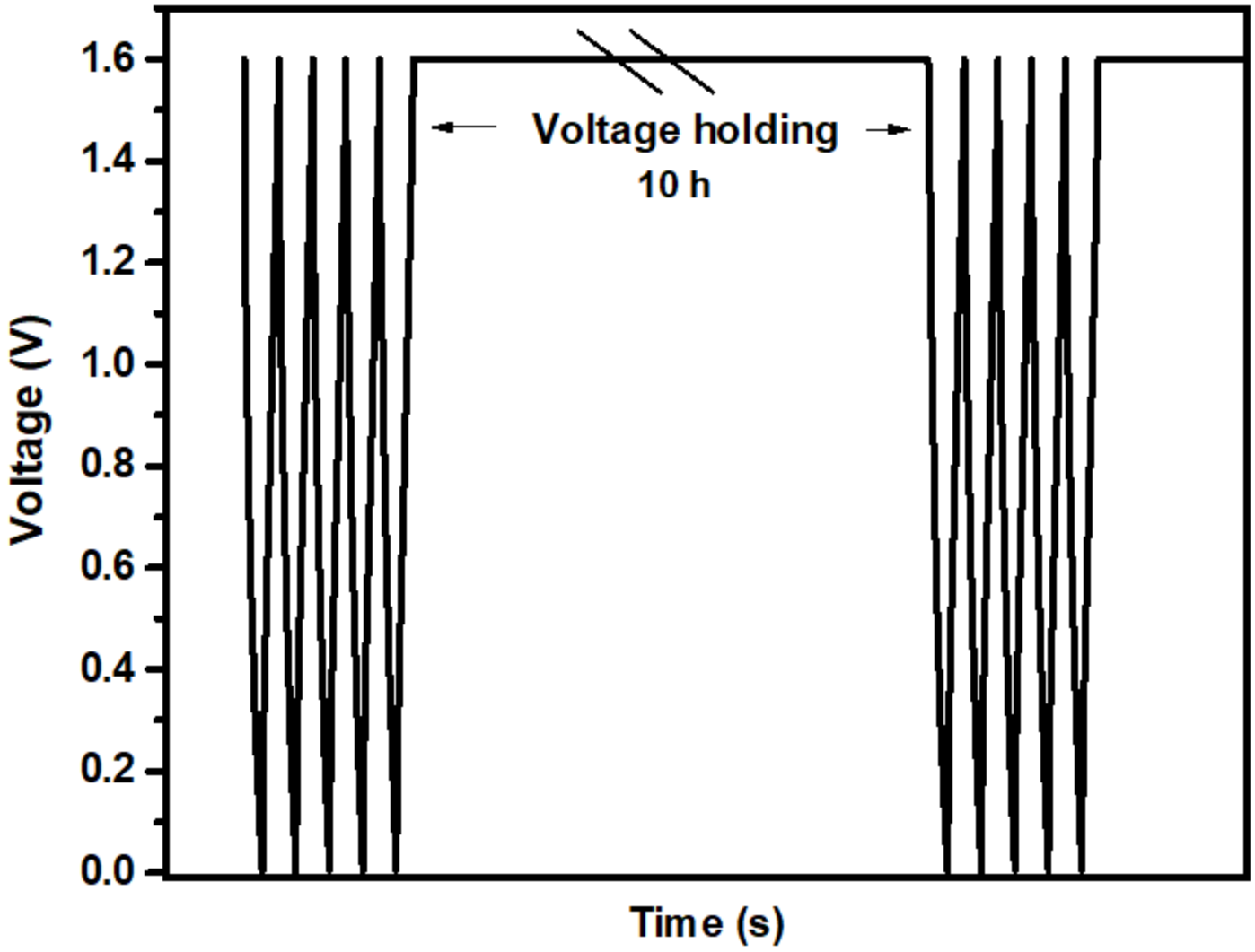

Figure 1

Illustration of the floating test experiment with 5 cycles of charge/discharge and 10 hours of voltage holding

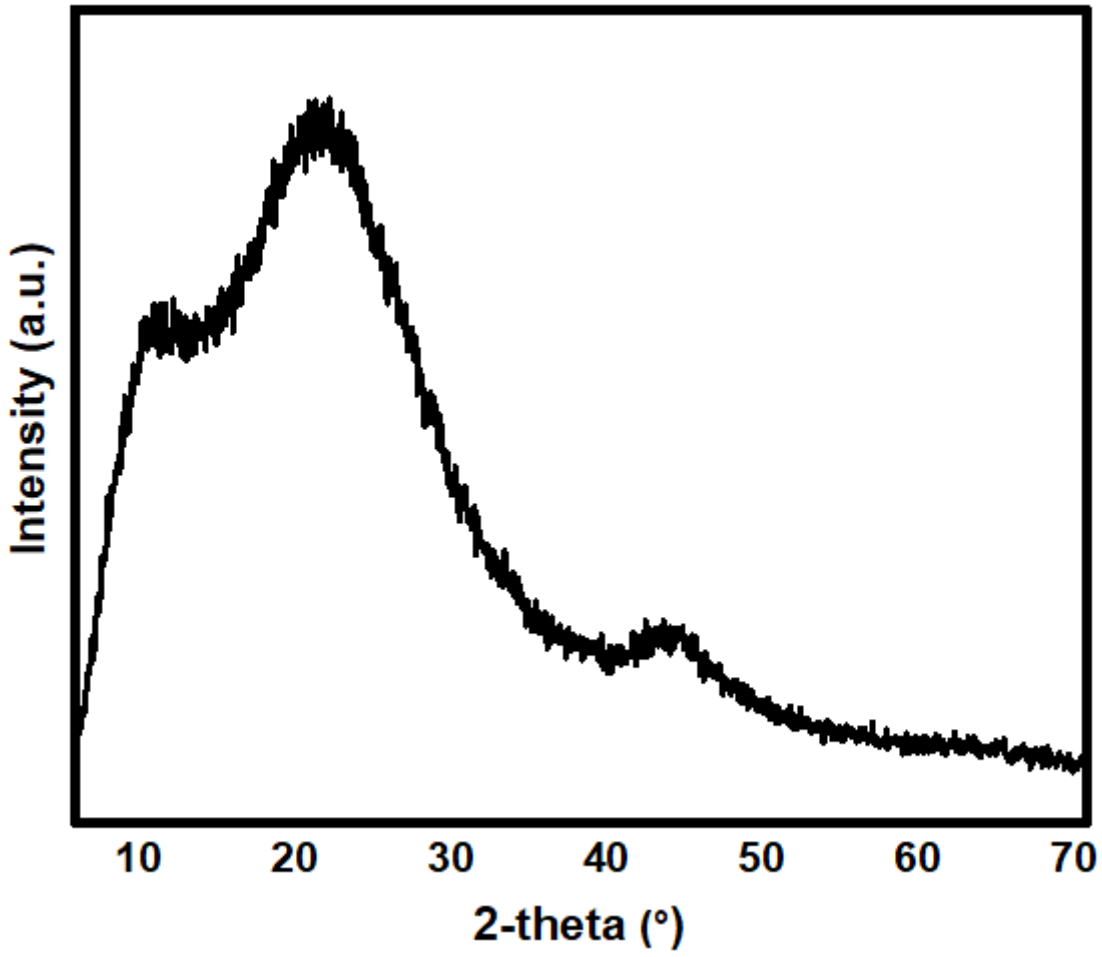

Figure 2

XRD diffractogram of the activated carbon

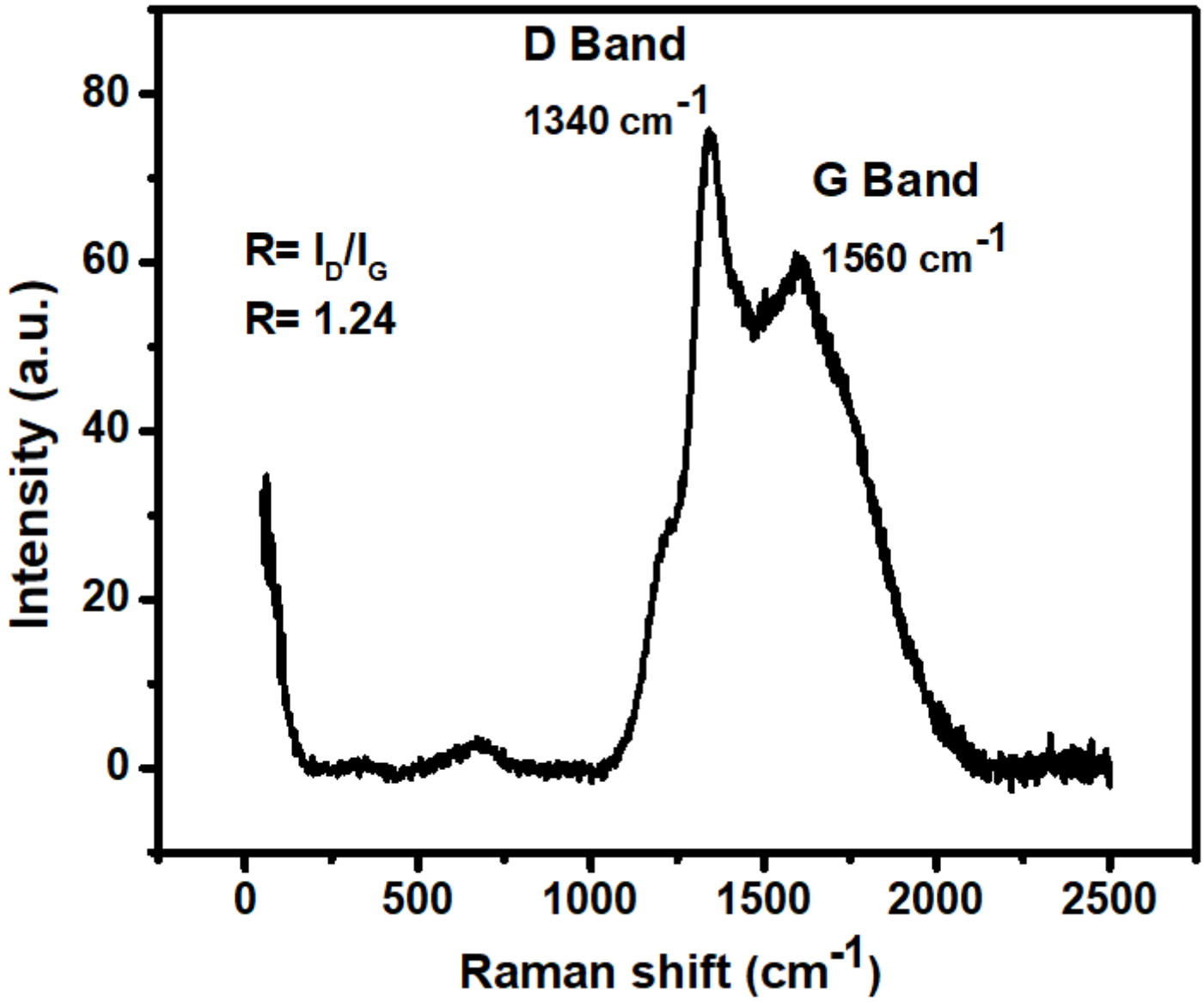

Figure 3

Raman spectra of the activated carbon heat treated at 800 °C.

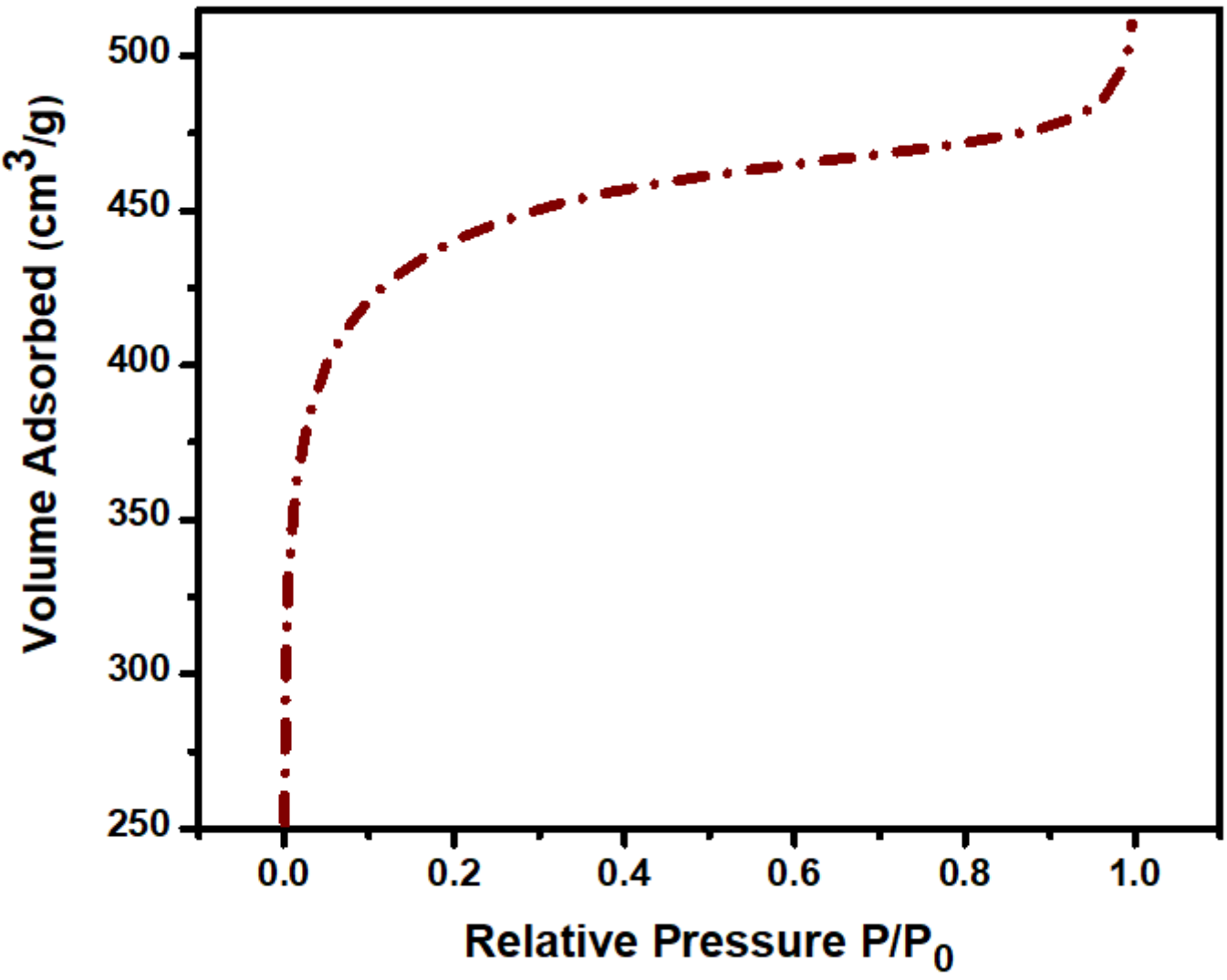

Figure 4

Nitrogen adsorption-desorption isotherms of the activated carbon material

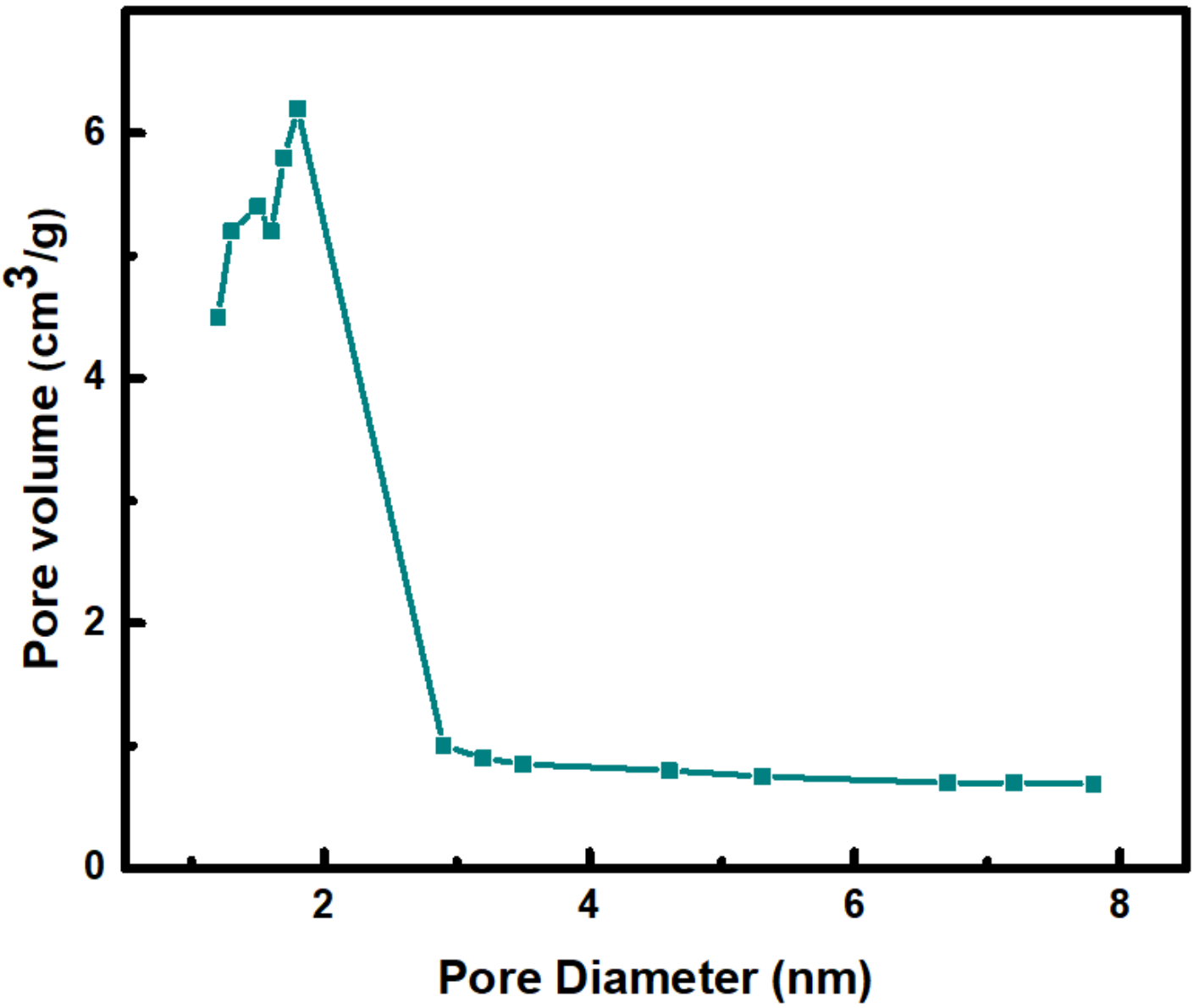

Figure 5

Pore size distribution of the activated carbon material heat treated at 800 °C.

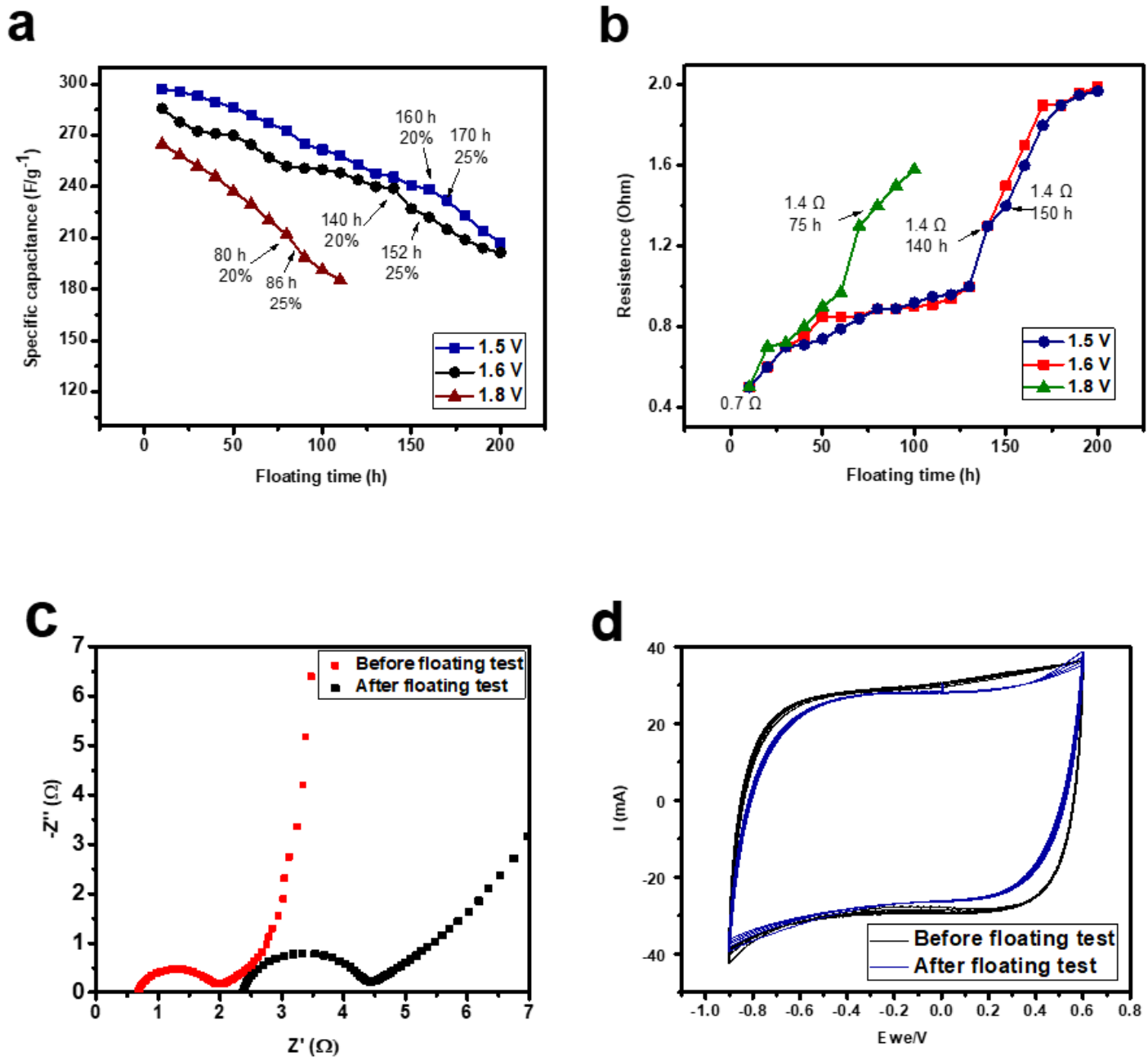

Figure 6

Electrochemical test of the full symmetric device: (a) capacitance decay in floating test at 1.8, 1.6 and 1.5 V (b) resistance increment in floating test at 1.8, 1.6 and 1.5 V (c) Nyquist plot of the two electrodes device before and after floating test at 1.5 V and (d) Cyclic voltammetry before and after floating test at 1.5 V